J. Fluid Mech. (1976), *vol.* 75, *part* 1, *pp.* 29–47
Printed in Great Britain

Observations on turbulent-drag reduction in a dilute suspension of clay in sea-water

By GISELHER GUST

Institut für Meereskunde an der Universität Kiel,
23 Kiel, Düsternbrooker Weg 20, Germany†

(Received 5 August 1975)

Hot-wire anemometer measurements have been made in a dilute sea-water/clay-mineral suspension. For fully developed turbulent flows in an open channel with a smooth mud (from the North Sea) bottom, mean streamwise velocity profiles were measured for Reynolds numbers between 5400 and 27 800 (i.e. non-eroding and eroding flow rates) and compared with Newtonian flows under the same experimental conditions. For the clay-mineral suspensions, measurements of the kinematic viscosity ν, Kármán's constant κ and the mean streamwise velocity $\overline{u}$ of the logarithmic layer seemed to verify a Newtonian flow structure. Although the distributions of concentration showed no substantial increase towards the wall, it was found that beneath this Newtonian core there existed a viscous sublayer whose thickness was enhanced by a factor of 2–5. The friction velocity u_* determined by the gradient method in the viscous sublayer was reduced by as much as 40 %. The mean flow structure exhibited an additional new layer in the region $10 < y^+ < 30$.

The measurements indicate that turbulent-drag reduction occurs for the experimental clay-mineral suspension at non-eroding and also at eroding velocities. Agglomeration of suspended clay-mineral particles is suggested as possible explanation of this phenomenon.

1. Introduction

Turbulent flows of fluid suspensions normally show non-Newtonian properties. Mechanical properties and anomalous flow behaviour of such non-Newtonian fluids have been studied for some time by rheologists and fluid dynamicists. The systems under investigation were mainly idealized suspensions or of a specific form important for some engineering problem (see, for example, Hinch & Ziabicki 1974).

On the geophysical scale, oceanographers, sedimentologists and hydraulic engineers have to consider two-phase systems consisting of cohesionless or cohesive sediments suspended in fresh water or in sea-water. For suspended sediments without cohesion a decrease in Kármán's constant κ with an increasing amount of suspended sediment was measured, but the flow remained Newtonian (Hunt 1954; Ippen 1971). Rheologic measurements showed properties of a

† Present address: University of Hawaii at Manoa, Department of Oceanography, 2525 Correa Road, Honolulu, Hawaii 96822.

Bingham-fluid (Einstein & Krone 1962; Pazwash & Robertson 1971) for cohesive suspended sediments in sea-water, while mean flow measurements in the logarithmic part of the turbulent boundary layer of such two-phase systems led to the conclusion of Newtonian flow structure (Terwindt, Breusers & Svasek 1968; Einstein & Krone 1962; Migniot 1968) and hence to the applicability of the universal law of the wall in sea-water/clay-mineral suspensions.

In contradiction to this assumption, the occurrence of turbulent-drag reduction by suspended clay minerals was suggested by Zandi (1967). Drag reduction by additives has become an important research field since Toms (1949) measured drag reduction in dilute polymer solutions in turbulent pipe flow (for reviews see Bark, Hinch & Landahl 1975). Nevertheless, convincing experimental results for drag reduction in clay suspensions are still lacking.

According to the author (Gust 1975), previous measurements of vertical mean velocity profiles and concentrations of suspended cohesive sediment in the logarithmic part of a tidal channel flow in the North Sea were not consistent with the universal law of the wall in a dilute sea-water/clay-mineral suspension. However, discrimination of the type of non-Newtonian flow was not possible because of the instruments' limitations. Owing to the contradictory available results and hypotheses about the turbulent boundary-layer structure of a cohesive sediment suspension over a hydraulically smooth mud bottom, a laboratory experiment was planned to clarify the validity of the universal law of the wall

$$U^+ = \kappa^{-1} \ln y^+ + C_1 \qquad (1)\dagger$$

and to verify the occurrence of drag reduction (dimensionless velocity $U^+ = \bar{u}/u_*$, $\bar{u}$ = local mean velocity; dimensionless wall distance $y^+ = yu_*/\nu$, y = vertical wall distance, ν = kinematic viscosity; C_1 = integration constant).

To achieve these goals, the experiment had to fulfil the following conditions.

(i) Simulation of tidal flow under controllable conditions.

(ii) Comparison of the boundary-layer structure of the two-phase flow with that of flows obeying the universal law of the wall under the same experimental conditions.

(iii) Use of a small velocity probe which works reliably also in the sea-water/clay-mineral suspension and detects the flow structure down to the viscous sublayer.

(iv) Experimental determination of all other variables in the law of the wall (viscosity, density and concentration of suspended sediment) for a proper non-dimensionalization of vertical mean velocity profiles and to check whether the distribution of concentration might cause a deviation from the law of the wall.

The experimental conditions and procedure used to meet these requirements are described in detail to confirm the results obtained.

† For Newtonian flows, Kármán's constant was found to vary in the range 0·36–0·41 and the integration constant C_1 to vary between 4·8 and 5·9 depending on the Reynolds number (see Tennekes & Lumley 1972, p. 176).

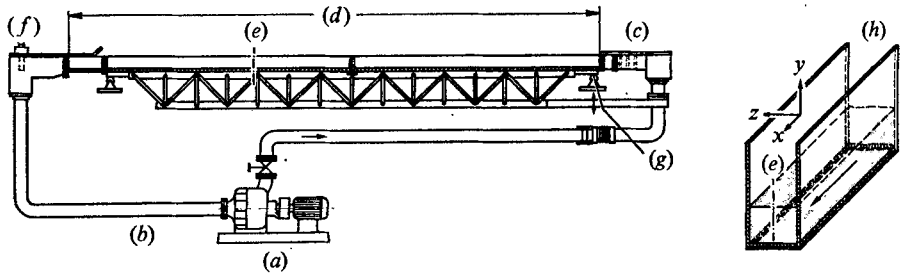

FIGURE 1. Sea-water resistant channel. (*a*) Centrifugal pump. (*b*) Recirculation system. (*c*) Inlet with mesh screens and honeycomb. (*d*) Measuring section. (*e*) Measuring point. (*f*) Outlet with thermostat unit. (*g*) Adjustment of channel's slope. (*h*) Channel cross-section.

2. Experimental equipment and procedure

The data reported here were taken in the turbulent boundary layers in three different hydraulically smooth flow systems (see § 4) in a sea-water resistant open channel (figure 1). The channel had a length of 400 cm, a height of 14 cm, a width of 8 cm and was filled with 60 l of fluid up to a height d of 6 cm. Thus a height/width ratio of 0·75 was obtained, where secondary currents could become important. The closed recirculation system contained a pump that transported the water into a 40 cm long inlet at the beginning of the test section. To achieve zero-pressure-gradient conditions, the test section could be tilted. All velocity measurements were taken 280 cm downstream of the inlet at the channel's base in the symmetry plane of the two vertical walls. At such a distance, which was 35 times the channel width, turbulent velocity profiles are fully developed provided that flow conditions in the entrance are uniform. This was achieved by a honeycomb and two fine mesh screens in the entrance. During operation, the (sea) water was heated by the pump to more than 30 °C. To establish stable measuring conditions, a thermostat unit in the outlet of the channel held the fluid temperature fixed at $34 \pm 0{\cdot}2$ °C. Important information on the flow conditions in the different flow systems was obtained by illuminating the measuring site from behind with diffuse light. Observing the channel's wall during the runs allowed estimation of the ranges of non-eroding channel velocities. Subsequently, light attenuation due to the suspended particles indicated that the clay concentration did not increase substantially towards the wall. From vertical light attenuation profiles heights were then selected at which to take suspension samples from the flows. Direct observation of the path of single suspended clay aggregates in the flow near the wall showed no influence of secondary currents.

The velocity measurements were performed by hot-wire anemometry (TSI, type 1050) with the probe 1265 W (TSI). Hot-film and hot-wire measurements show severe limitations if carried out in sea-water. Frey & McNally (1973) state in their investigation of the applicability of hot-film probes in sea-water for turbulence measurements the following disadvantages.

(i) Downward drift in probe sensitivity.

(ii) Short life span of probes.

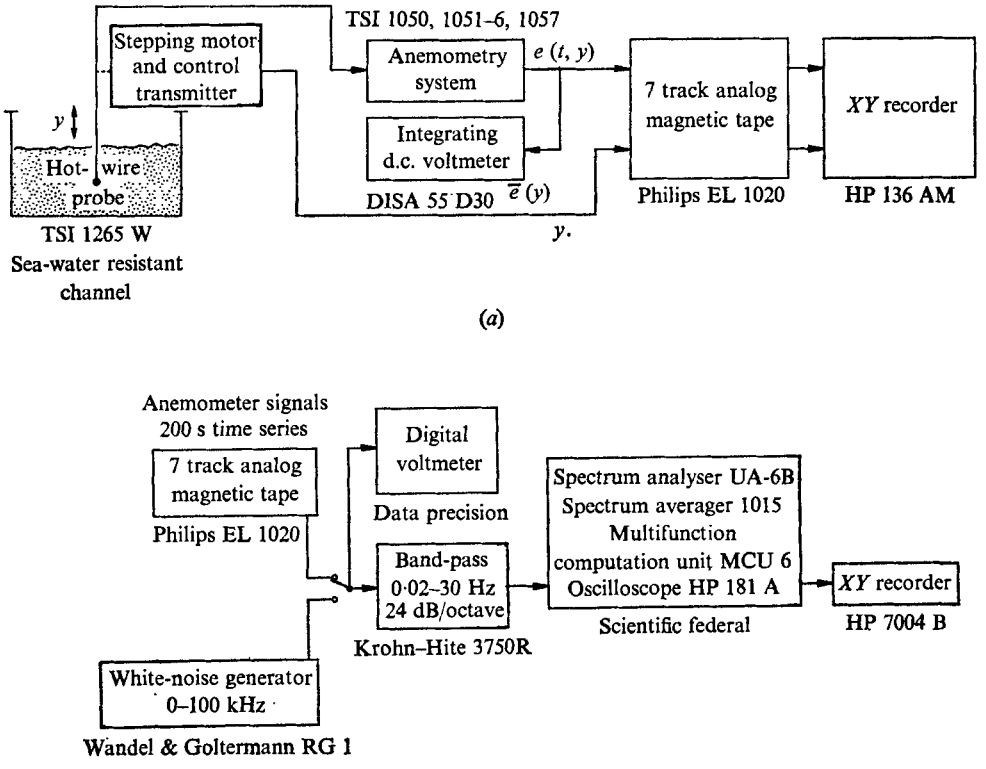

FIGURE 2. Block diagrams. (*a*) Measurement of local streamwise velocities (y vertical wall distance). (*b*) Spectrum analysis.

(iii) Bad directional sensitivity forbidding the observation of the three spatial components of flow.

(iv) Ambiguities in the value of the exponent in King's law.

In contrast to the quartz-coated platinum hot-film probes checked by Frey & McNally (1973) the author's measurements were performed with a coated hot-wire probe. Here the hot wire is imbedded in Al_2O_3 and has outer metal protection. This construction makes the probe less fragile but still gives sufficiently short thermal response times (see §3) with an electrically insulated wire. The probe could be used in dirty fluids as it withstood strong mechanical impacts. It had a diameter of 0·4 mm. Although this diameter is relatively large, with the single-wire probe set normal to the mean flow the mean longitudinal velocity component $\bar{u}$ and longitudinal turbulent velocity fluctuation u' could be measured down to the bottom; this was also possible in the two-phase flow. Depending on the free-stream velocity U, pools were sometimes observed in the quartz sand bottom of the Newtonian flow system when the distance of the probe was smaller than 0·5 mm. Therefore no measurements were analysed with a wall distance of the probe smaller than 1 mm except for the suspension flow with a free-stream velocity U of 7 cm/s, for which data from a position 0·5 mm above the bottom were processed.

Block diagrams of the electronic equipment used in this experiment are shown in figure 2. The probe was mounted on a manipulator which was positioned vertically with an accuracy of $\frac{1}{20}$ mm and gave a height read-out on a digital voltmeter DX 703 A (ITT) and on an X, Y recorder 136 AM (HP). The non-linearized anemometer signals were registered by this recorder and were also recorded on a 7 track analog magnetic tape EL 1020 (Philips). An integrating d.c. voltmeter 55D30 (DISA) with a time constant of 10 s was used to compute from the time series of 70 s and 200 s duration the mean longitudinal velocity component $\overline{u}$. Spectral analysis of the fluctuating longitudinal velocity component was performed by an analog spectrum analyser UA-6B with a spectrum averager 1015 and multifunction computation unit MCU6 (Federal Scientific). The d.c. and higher frequency components were cut off at the input terminal by a band-pass filter ranging from 0·02–30 Hz, 24 dB/octave (Krohn-Hite, Type 3750 R). The frequency range analysed was between 0·1 and 30 Hz. The turbulence data were analysed to give an independent test of the frequency response of the probe 1265 W and, hence, properly averaged values of the mean longitudinal velocity $\overline{u}$.

Contamination of the probe in the two-phase flow was avoided by cleaning it with a smooth brush after each time series. The temperature of the fluid was continually checked by a mercury thermometer with a 0·1 °C scale, which showed no variations in temperature larger than those allowed by the thermostat unit.

Water samples of volume 25 ml were taken at the measuring site from the suspension flows to determine the distributions of viscosity, density and concentration. Because of light attenuation, which indicated nearly homogeneous concentration profiles down to the wall, for Reynolds numbers Re_U of 8400, 13 100, 17 000 and 21 600 the samples were taken at heights between 1 and 4 cm above the wall in steps of 1 cm. The viscosity was then measured by an Ostwald viscosimeter and the density by a mechanical oscillator constructed by Kratky, Leopold & Stabinger (1969). Concentrations of suspended sediments were determined by sedimentation of the samples, filtering them and weighing the remainder and also from the difference in density from that of clean sea-water.

Furthermore, a phase contrast microscope (Leitz) was used to measure the size of the clay aggregates by microphotos. These aggregates, after settling, were formed in sedimentation chambers from the samples of the suspension flows.

3. Calibration of the anemometry system and tests

The calibration of the hot-wire anemometry system was performed in a rotating tank. Variations in the hot-wire signals due to contamination and possible changes in the coefficient α of heat transmission in the various fluids were checked by calibrating the probe in fresh water, sea-water and sea-water/clay suspensions. Within the range of accuracy, the calibration curve remained the same for the different fluids. The only significant parameter was temperature.

Contamination of the probe by clay-mineral particles reduced the output voltage of the anemometer (which lay between 7 and 10 V in the velocity range 0–35 cm/s) by 0·2 V at a constant velocity of 15 cm/s during a 10 min measuring

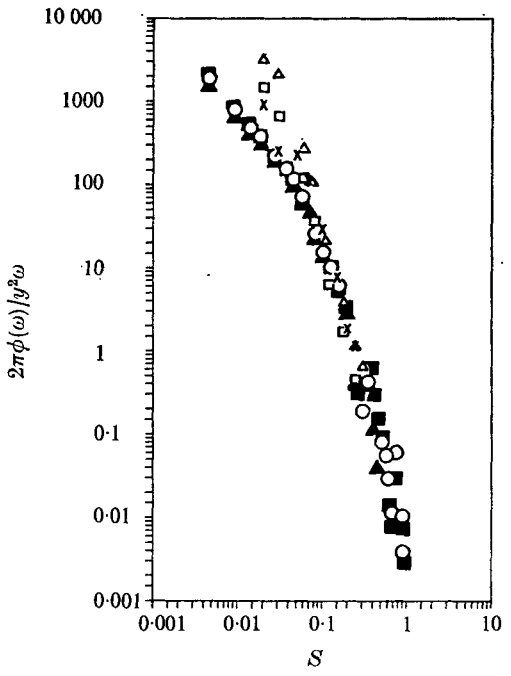

FIGURE 3. Non-dimensionalized spectra of the streamwise fluctuating velocity within the viscous sublayer.

	Bakewell & Lumley			Clay suspension		
	■	○	▲	□	△	×
y^+	5	2·5	1·25	9	4·5	1·5

(For co-ordinates (S, ϕ) see Bakewell & Lumley 1967, equations 7 and 8.)

time. To avoid contamination, time series at a given height for measuring the mean longitudinal velocity or the longitudinal velocity fluctuations in the channel were thus limited to 70 s or 200 s, respectively.

The anemometer signals were linearized by an approximating polynomial of fifth order, which fitted the calibration curve with deviations of less than 5 %. No drift of the calibration curve occurred during the measurements; this was proved by recalibrating the probe at the beginning and end of each measuring series for the different flow systems.

For velocity measurements in turbulent flows the frequency response of the probe must be known to evaluate proper mean flow values and turbulence intensities. Using the square-wave method described by Freymuth (1967) with an external square wave of 10 Hz (0·7 V amplitude) fed to the anemometer and an overheat ratio of 1·12, the -3 dB frequency response of the probe in water with no flow was 26 Hz. Thus, for the flows in the channel with Reynolds numbers $Re_U = Ud/\nu$ of the order of 10^4 the probe showed a sufficiently high frequency response to measure the expected longitudinal mean velocities (McQuivey & Richardson 1969). For Reynolds numbers $Re_U = 5400$ and 13 100 no significant difference was detected in the turbulence spectra at different heights in the

logarithmic part of the two-phase flows as compared with the one-phase flows.

The spectra compared had a 99 % confidence interval of only 3 dB, because the measuring intervals in the sea-water/clay-mineral suspension were limited to a maximum of 200 s in order to avoid possible contamination of the probe.

A further check on the applicability of the probe 1265 W in turbulent flow of dilute clay-mineral suspensions was performed by comparing turbulence spectra obtained in the viscous sublayer at a Reynolds number $Re_U = 5400$ with those of Bakewell & Lumley (1967) for turbulent glycerine pipe flow at $Re_U = 8700$. They showed that for $y^+ = 1{\cdot}25$, $2{\cdot}5$ and 5 a non-dimensionalized spectrum of the streamwise fluctuating velocity u' within the viscous sublayer indicated a linear dependence of u' on the dimensionless co-ordinate normal to the wall. The author's measurements of the streamwise fluctuating velocity u' were taken at $y^+ = 1{\cdot}5$, $4{\cdot}5$ and 9. Using the same dimensionless energy and frequency co-ordinates, the dimensionless spectrum of u' in the turbulent suspension flow showed qualitative agreement with that of Bakewell & Lumley in the comparable frequency range, as demonstrated in figure 3. As shown in figure 3, the energy-containing part of the spectrum for the clay suspension is raised. It is an open question whether this result can be interpreted as a different turbulence structure in the viscous sublayer of the non-Newtonian two-phase flow.

Additional errors in hot-wire and hot-film measurements in turbulent flows are possible. For a single-wire probe oriented parallel to the wall and normal to the flow, an estimate of the error in the u' component due to v' fluctuations can be made by considering Klatt's (1973, equation 5 N) third-order approximation:

$$\frac{\overline{u'^2}}{\overline{u}^2} = \left(\frac{\overline{u'^2}}{\overline{u}^2}\right)_{\text{meas}} \left\{1 + \frac{1}{(\overline{u'^2}/\overline{u}^2)_{\text{meas}}} \left[a^2 \frac{\overline{u'w'}}{\overline{u}^2} + 2k\left(\frac{\overline{u'^2}}{\overline{u}^2}\frac{k\overline{v'^2}}{4\overline{u}^2}\right)\frac{\overline{v'^2}}{\overline{u}^2}\right]\right\}. \tag{2}$$

For the probe, a describes deviations from the cosine law and k describes the sensitivity to vertical velocity fluctuations v'. Setting $a = 0$ and $k = 1{\cdot}4$ (according to Klatt) the maximum error for the turbulence data was then estimated to be 5 % for distances $y^+ < 10$ and less than 1 % otherwise, using Laufer's (1954) turbulence data on a two-dimensional turbulent flow. The error due to the influence of the wall on the heat transfer from the hot wire was disregarded, as only streamwise velocity data at distances no closer than 0·5 mm from the wall were considered.

Mean flow data measured by a single-wire probe also depend on the turbulence intensity. An error of less than 1 % was given for the measurements by Klatt's (1973, equation 4) formula for this type of error,

$$\overline{u} = \frac{\overline{u}_{\text{meas}}}{1 + \frac{1}{2}k\overline{v'^2}/\overline{u}^2}, \tag{3}$$

and Laufer's (1954) turbulence data.

Because of contamination of the probe in the clay-mineral suspensions, the anemometer signals decreased by 0·2 V over measuring intervals of about 10 min. This effect, which resulted in a relative error of 40 % for velocities higher than 15 cm/s, was avoided by choosing averaging times of 70 s, although for low

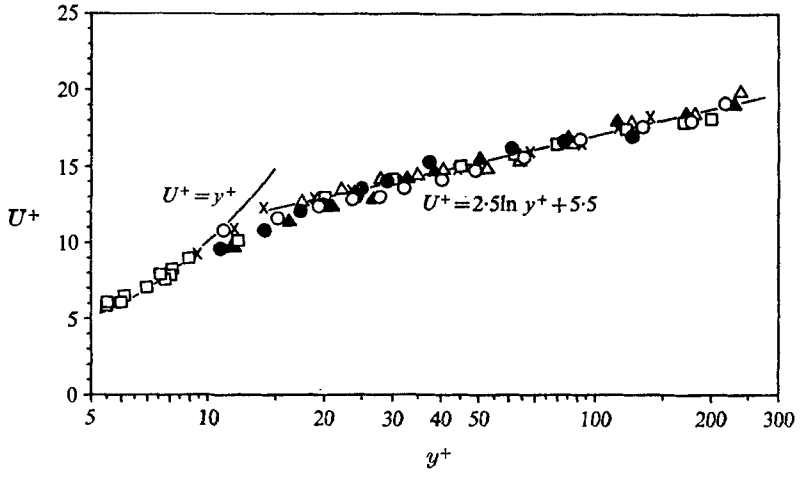

FIGURE 4. Mean streamwise velocity distribution in Newtonian flow systems ($U^+ = \bar{u}/u_*$, $y^+ = yu_*/\nu$).

Oil channel	Re_U		Re_U
(Eckelmann 1970)		Quartz sand/fresh water	
□	8 200	×	5 600
Lucite/fresh water		●	10 400
○	10 400	▲	15 300
△	15 300		

Reynolds numbers and at small wall distances this averaging time was relatively short. Therefore, mean velocity measurements near the wall were partly repeated and resulted in reproducible anemometer output signals. Maximum measured deviations of the averaged anemometer output signals were then 50 mV at voltages ranging between 7 and 10 V. This was equivalent to a possible maximum error of 10 % for mean velocities in the range 0–25 cm/s, caused by temperature variations of ± 0·2 °C in the fluid and changes in the flow structure due to slightly varying pumping rates. As shown in figure 4, minor deviations of the measured mean velocity profiles of the Newtonian flows from the law of the wall [equation (1)] and from velocity profiles taken in an oil channel under refined measuring conditions in the same Reynolds number range (Eckelmann 1970) allow the conclusion that the relative error in the measurements was considerably less than 10 %.

4. Smooth channel flow systems

To check the universal law of the wall in sea-water/clay-mineral suspensions, three different smooth flow systems were set up and compared under equivalent experimental conditions.

The Newtonian flow system using lucite and tap water with a smooth bottom resulting in roughness Reynolds numbers $Re_{k_s} = u_* k_s/\nu$ (k_s = height of roughness elements) less than 2 for the flow conditions in question was used to check whether the universal law of the wall was obtained for the turbulent flows in the

open channel. This was proved by comparing measured mean velocity profiles with the theoretical curve $U^+ = 2{\cdot}5 \ln y^+ + 5{\cdot}5$ and with data obtained by Eckelmann (1970), as demonstrated in figure 4.

For the flow system using fine quartz sand and fresh water the bottom of the channel's test section was filled with sand up to a height of 0·8 cm. The quartz sand was taken from the beach of the Baltic at Heidkate and contained a small amount of feldspar. The mean diameter of the quartz grains was about 200 μm, which resulted in a roughness Reynolds number Re_{k_s} of 3 for the maximum channel velocity U of 25 cm/s. The velocity profiles of this natural Newtonian smooth flow system served as reference profiles for the measurements in the sea-water/clay-mineral suspension. The mean flow data verified that the flow in the quartz-sand/tap-water system remained smooth for the entire non-eroding velocity range (7–25 cm/s) and did not develop to the transition range.

The mud bottom and the sea-water/clay-mineral suspension were taken from a tidal flat on the west coast of Schleswig-Holstein (Island Nordstrand). A near-surface sample of the mud was subjected to grain-size analysis with the result that more than 60 % of the particles had a size less than 50 μm and the maximum size of single particles was 150 μm. Thus smooth flow conditions were obtained. When the channel's entire bottom was coated with mud pieces from the field, the samples maintained an undisturbed structure and their original surface.

The field conditions to be examined were classified from a tidal flow from a closed bay after slack water without erosion. Corresponding measuring conditions in the laboratory were obtained by using unfiltered sea-water from the field site in addition to the original mud bottom.

The distribution of concentration of the suspended cohesive sediment was measured in two different ways. Density measurements of the sea-water/clay-mineral suspension and of filtered sea-water were made. The amount of suspended sediment then resulted from the difference in density. The device used for these measurements was developed and described by Kratky *et al.* (1969). Its measuring principle is the change in frequency when an oscillating hollow glass pipe is filled with fluids of different density. The density of sea-water/clay-mineral suspensions with concentrations of suspended cohesive sediment of 1 g/l could be measured to an accuracy of one part in 10^5.

While taking the samples from the flow the formation of aggregates in the suspension and temperature fluctuations of $\pm 0{\cdot}2$ °C in the fluid resulted in a varying density. Thus a limited accuracy of only one part in 10^4 was obtained for the density measurements. An upper limit of 380 mg/l was found by this method for the concentration of the suspended cohesive sediment at non-eroding channel velocities. At eroding channel velocities $U = 32$ and 36 cm/s the concentration of suspended sediment was of the order of 1 g/l. Table 1 shows the concentrations obtained from the density measurements. They are compared with concentration values obtained from filtering the water samples and weighing the remainder.

For a proper interpretation of the mean flow results for the clay suspension (§ 5) further hydrodynamic parameters of the dilute water/clay-mineral suspension had to be measured.

Re_U	Height above wall (cm)	Density (g/cm³) *A*, suspension *B*, clean sea-water	Concentration (mg/l) Difference in density *A*–*B*	Concentration (mg/l) Filtering and weighing	Kinematic viscosity at 34 °C [(cm²/s) × 10²]	Estimate of kinematic viscosity if 'Newtonian viscous-sublayer thickness' holds [(cm²/s) × 10²]	Micro-photo
		Water samples from non-eroding suspension flows					
8 500	1	*A* 1·02261	130	—	0·778	1·43	×
	2	—	—	—			
	3	*B* 1·02248	—	114			
	4	*A* 1·02263	150	—			
13 100	1	*A* 1·02293	380	268	0·778	1.3	×
	2	*B* 1·02255	—	196			
	3	—	—	—			×
	4	*A* 1.02275	200	152			×
17 000	1	*A* 1·02273	130	—	0·778	1.12	
	2	*A* 1·02272	120	—			
	3	*A* 1·02276	160	—			
	4	*B* 1·02260	—	—			
21 600	1	*A* 1·02287	180	249	0·778	1·75	×
	2	*B* 1·02269	—	162			
	3	—	—	—			
	4	*A* 1·02298	290	—			
Filtered sea-water	–	—	—	—	0·778	—	—
		Other samples					
Sea-water/clay suspension				500	0·78		
Eroding channel flows				2160	0·8		
				4570			
				10400	0·969		
Tap water					0·746		
Distilled water					0·740		

TABLE 1. Concentration and viscosity measurements

X-ray analysis of the 2 μm fraction of the mud and of a suspension sample from the field site yielded more than 50 % Illite and less than 5 % Chlorite and mixed crystals, the remaining part being Kaolinite. The size of the single clay particles was mainly less than 1 μm.

Clay minerals build up an electrical double layer in dilute electrolytes (e.g. sea-water), thus forming various types of aggregate (see van Olphen 1963). Figures 5 (*a*)–(*d*) (plates 1 and 2) are microphotos of sedimented aggregates from 1·7 ml sedimentation chambers. They were taken by an inverted microscope equipped with phase contrast. Figures 5 (*a*) and (*b*) refer to samples from heights of 1 and 2 cm above the bottom respectively. The microphotos of samples taken at 3 and 4 cm above the wall were similar to those in figures 5 (*a*) and (*b*). Therefore,

throughout the whole water column the clay suspension consisted of such agglomerations. Figure 5 (*c*) shows aggregates from a height of 3 cm in a suspension flow with a Reynolds number of 8500, while figure 5 (*d*) was taken from a sample at the same height in a suspension flow with a Reynolds number of 21 600. The size distribution of the aggregates could not be determined under experimental flow conditions. For the agglomerations which were deposited in the sedimentation chambers an upper limit of 60 μm was found. On the microphotos shells of diatoms with a size of about 20 μm were also detected. Hence the organic contents of two suspension samples were determined to be 6·4 % and 7 % respectively with a C/N-ratio of 10 by means of a carbon–nitrogen analyser (Hewlett & Packard Type 185 B).

Viscosity of the suspension samples was measured by an Ostwald viscosimeter at the temperature in the channel. The measuring volume was 2 ml, and the Reynolds number based on the diameter of the capillary tube and mean velocity was 200. The shear rate $d\bar{u}/dr$ was 240 s^{-1}. If the increase in the kinematic viscosity ν due to added cohesionless sediments is estimated by means of the formula of Einstein (1906) an increase of 0·5 ‰ should be expected for a concentration of suspended sediment less than 380 mg/l. Influence of electroviscosity as described by the formula of von Smoluchovskij (1921) could not be considered. For all samples the kinematic viscosity ν from non-eroding flows of the sea-water/clay-mineral suspension was measured experimentally to be $0{\cdot}778 \times 10^{-2}$ cm^2/s. Thus no deviations were found from the filtered sea-water's viscosity within the limit of accuracy of 0·5 % (see table 1). For clay concentrations of 2·16 and 4·57 g/l the increase in the kinematic viscosity ν was then measured to be 3 %, while for a concentration of 10·4 g/l it was 25 %.

5. Results: boundary-layer structure and friction velocity u_* of the sea-water/clay-mineral suspension

From the measurements of the purely hydrodynamic parameters the flow systems compared do not appear to deviate from a Newtonian smooth flow structure. The mean longitudinal velocity data for the lucite and tap water system and for the fine quartz sand and tap water system in fact fulfilled the Newtonian expectations, as is shown in figure 4. On the other hand, all mean flow measurements of the sea-water/clay-mineral suspension yielded deviations from the universal law of the wall. In figure 6 an example of this is shown. Turbulent flows of comparable Reynolds number for the three flow systems exhibit a logarithmic region with same mean streamwise velocities. For the clay suspension, the subsequent viscous sublayer unexpectedly thickens to 5 mm above the mud bottom while for tap water it extends to about 1 mm. For all measurements in the sea-water/clay-mineral suspension for non-eroding and eroding free-stream velocities U between 7 and 36 cm/s the mean velocity profiles exhibited a 'Newtonian plug' (logarithmic part with slope according to the law of the wall), but the thickness of the viscous sublayer was increased by a factor varying between 2 and 5.

In Newtonian smooth flow, mean velocity data for the logarithmic region, its

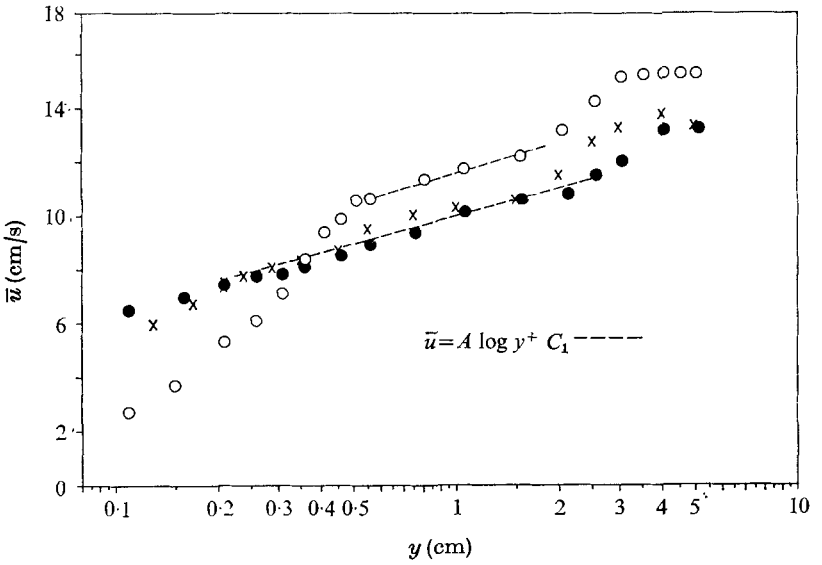

FIGURE 6. Mean streamwise velocity distributions. Slope $A = (u_*/\kappa) \times 2{\cdot}3$ with u_* from (1) and $\kappa = 0{\cdot}4$.

Newtonian		Re_U	A
Lucite/fresh water	●	10 400	3·85
Quartz sand/fresh water	×	10 400	
Non-Newtonian			
Mud bottom/clay suspension	○	11 600	3·45

slope and the thickness of the viscous sublayer are coupled by the friction velocity u_*, Kármán's constant κ and the kinematic viscosity ν. For the fresh-water flow systems, the measured mean velocity profiles were consistent with the law of the wall [equation (1)]. The experimentally determined thickness conformed with the viscous-sublayer thickness δ estimated from

$$\delta \sim 12\nu/u_*. \tag{4}$$

Now for the suspension flows Kármán's constant κ remained 0·4 (κ was given by the invariant slope of the logarithmic region). Then using the friction velocity u_* computed from the law of the wall [equation (1), now labelled $u_{*\log}$] and the kinematic viscosity ν of the dilute clay suspension (table 1) in (4) resulted in discrepancies in the thickness of the viscous sublayer compared with the direct measurements.

Now a thickened viscous sublayer could be compatible with the universal law of the wall if an increase in clay concentration in the viscous sublayer towards the wall gives a higher value of the kinematic viscosity ν at the bottom than in the flow. Under this assumption, the wall value $\nu_{y=0}$ of the kinematic viscosity must then be increased for the experimental suspension flows by a factor of at least 1·4 compared with the flow value. Such an apparent viscosity of $\geqslant 1{\cdot}12 \times 10^{-2}$ cm^2/s at 34 °C was not even measured for a sea-water/clay suspension (aggregated) with a clay concentration of $\sim$ 10 g/l. Then the increase in

		Logarithmic layer				Viscous sublayer		
U (cm/s at $d = 6$ cm)	$Re_U = \frac{Ud}{\nu}$	δ_{log} (cm)	$\bar{u}$ (cm/s)	at y (cm)	u_{*log} [equation (1)]	δ_{visc} (cm)	$d\bar{u}/dy$ (s^{-1})	u_{*visc} [equation (5)]
7	5 400	2·5	5·3	1·0	0·35	0·55	9	0·28
11	8 500	2·5	9·5	2·0	0·53	0·44	16	0·39
14	10 800	1·5	9·1	0·4	0·64	0·25	32	0·50
15	11 600	2·0	12·0	1·5	0·68	0·50	20	0·43
17	13 100	1.5	12·5	1·5	0·70	0·30	32	0·52
18	13 900	2·0	11·6	0·5	0·76	0·40	29	0·48
22	17 000	1·5	16·0	1·4	0·88	0·20	57	0·67
27	21 600	1·0	22·2	1·0	1·22	0·28	67	0·75
32	24 600	2·5	28·4	2·0	1·41	0·25	93	0·86
36	27 800	1·5	28·9	1·0	1·55	0·20	120	0·98

TABLE 2. Boundary-layer data for clay suspension flows. d, water depth; δ_{log}, thickness of logarithmic layer; δ_{visc}, thickness of viscous sublayer; $\bar{u}$, local mean velocity; U, surface velocity.

kinematic viscosity ν was 25 %. In contrast to this the actual concentrations in the non-eroding flows were less than 500 mg/l (see table 1), and by direct observation of the light attenuation profiles no substantial increase in concentration was detected in the viscous sublayer towards the wall. For the flows with a Reynolds number Re_U of 8500 and 13 100 a reduced amount of suspended particles in the viscous sublayer was even observed. Thus for the wall value $\nu_{y=0}$ of the kinematic viscosity the same value was taken as was obtained for the samples 1 cm (and higher) above the bottom, where the clay suspensions also consisted of agglomerations. As a consequence, the non-dimensional thickness of the viscous sublayer was not comparable to the universal value (~ 12), even when the actual friction velocity u_{*visc} (see below) was used.

In addition, from the law of the wall, the friction velocity $u_* = (\tau_0/\rho)^{\frac{1}{2}}$ (ρ = fluid density) can be computed from the experimentally determined vertical mean velocity gradient in the viscous sublayer:

$$u_* = (\nu\, d\bar{u}/dy)^{\frac{1}{2}} \quad \text{(now labelled } u_{*visc}\text{)}. \tag{5}$$

This was done for the experimental flows. The wall shear stress τ_0 was not determined from the angle of tilt of the channel because of the non-uniform distribution of τ_0 at the bottom and the effect of the side walls.

For Newtonian flows without a horizontal pressure gradient, the ratio u_{*visc}/u_{*log} varies between 1 and 0·8 (Kemp & Grass 1967). Schraub & Kline (1965) have shown that this ratio depends on the horizontal pressure gradient and also on the Reynolds number.

In the experiment it was found that for the Newtonian flows without a horizontal pressure gradient the friction velocities coincide when computed by the law of the wall and by the gradient method. This did not apply to the clay suspension flows. The values of u_{*visc} were then drastically reduced as compared with u_{*log}, and the ratio u_{*visc}/u_{*log} varied between 0·6 and 0·8 (see table 2),

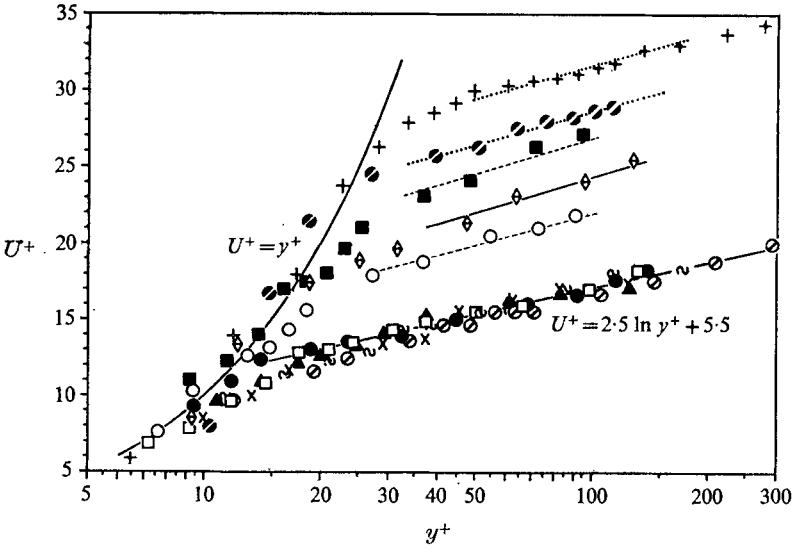

FIGURE 7. Mean streamwise velocity distributions.

Newtonian Quartz sand/fresh water Re_U		Non-Newtonian flow systems Mud bottom/clay suspension Re_U		
5 600	●	5 400	○	non-eroding
8 000	□	8 500	■	non-eroding
9 600	×			
10 400	▲	10 800	◇	non-eroding
15 300	~	24 600	+	eroding
20 000	⊘	27 800	◪	eroding

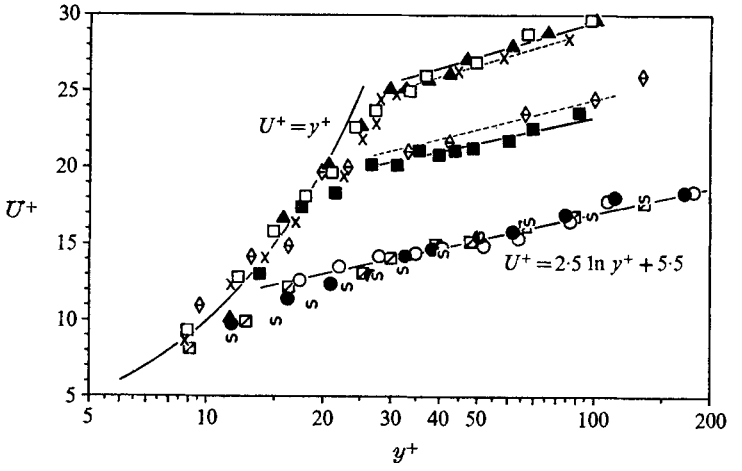

FIGURE 8. Mean streamwise velocity distributions.

Newtonian Lucite/fresh water Re_U		Non-Newtonian flow systems Mud bottom/clay suspension Re_U	
15 300	○	11 600	×
Quartz sand/fresh water		13 100	◇
12 000	~	13 900	□
12 900	◪	17 000	■
15 300	●	21 600	▲

although the experimental conditions were the same for all turbulent flows. Consequently $u_{*\,\mathrm{visc}}$ was used for drawing dimensionless velocity profiles from the suspension mean flow data.

In figures 7 and 8 these dimensionless mean velocity profiles for the Newtonian and non-Newtonian flows are shown in groups with comparable Reynolds numbers. In contrast to the Newtonian flows, the velocity profiles of the sea-water/clay-mineral suspension do not fit the universal law of the wall, but give a system of curves with different thickened viscous sublayers and an invariant slope of the logarithmic part. No systematic Reynolds number dependence is exhibited by this system of curves, and the concentration measurements of the suspended clay minerals (limited by experimental difficulties) do not allow correlation of the non-dimensional velocity profiles with the concentration of the suspended clay minerals. Currently it is not known which parameters govern this system of curves, but it is assumed that in addition to the concentration of the clay suspension the type of clay mineral and the shear rate of the flow play a dominant role.

6. Discussion

The experimental results on the boundary-layer structure of the sea-water/clay-mineral suspension described in the previous section show that the universal law of the wall is not valid for this particular turbulent two-phase flow. The dimensionless velocity profiles (figures 7 and 8) of the clay suspension deviate from the law of the wall in the region $10 < y^+ < 30$. An additional layer seems to be inserted there, shifting the 'Newtonian core' of the logarithmic layer.

This type of boundary-layer structure is known for smooth turbulent flows exhibiting drag reduction by additives. In figure 9, dimensionless velocity profiles for the clay-mineral suspension are compared with experimental mean velocity profiles for drag-reducing polymer flows. The similarity of the flow structures clearly demonstrates the occurrence of drag reduction for the clay-mineral suspension.

For the suspension flows, the pumping rate had to be reduced to obtain the same mean velocity profiles as in the fresh-water flows. Then the slope decreased for the same flow rate, thus manifesting drag reduction. In figure 10, mean velocity profiles were used to express the wall shear stress τ_0 in terms of the friction factor $f = 8(u_*/\overline{U})^2$ ($\overline{U}$ = mean channel flow), which is a function of the Reynolds number $Re = 4\overline{U}R/\nu$ (R = hydraulic mean radius) and the (unknown) clay parameters causing drag reduction. Therefore no curve may be drawn from the data points for the suspension flows, but their downward shift from the pure-water values demonstrates the occurrence of drag reduction. The data points obtained from the experiment with the sand bottom and fresh-water system are not compared with any pipe resistance laws. Resistance studies of smooth open channels have shown that the friction factor then depends on shape and slope of the individual channel (Jayaraman 1970).

Drag reduction in the flow of liquid–solid suspensions in pipes has been reported for water suspensions of ground wood and wood pulp, nylon fibres, rayon fibres, asbestos fibres and derived products, and clay minerals (see Radin, Zakin &

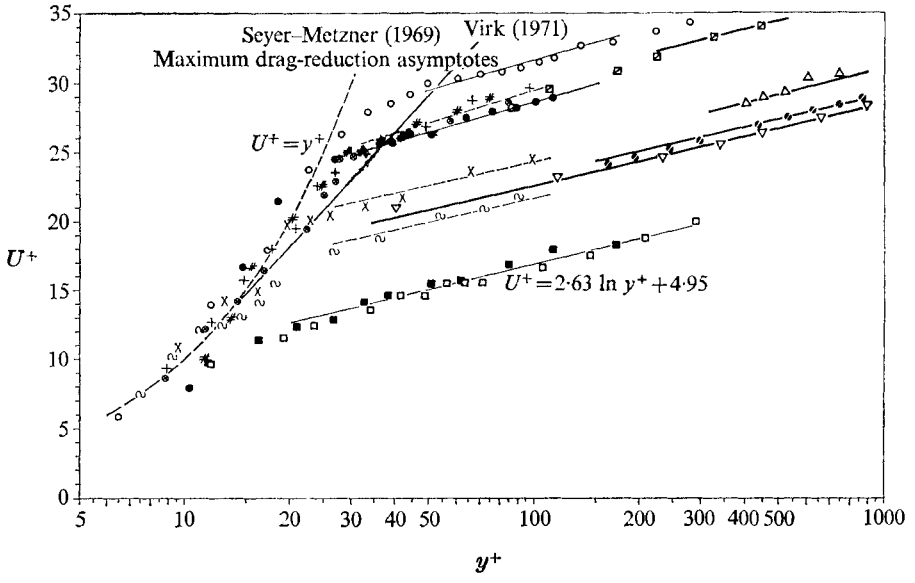

FIGURE 9. Drag-reduction data for experimental clay-mineral suspension and polymer flows (from Virk 1971, figure 2).

Quartz sand/fresh water	Re_U
■	15 300
□	20 000
Mud bottom/clay suspension	
~	5 400
⊗	11 600
×	13 100
+	13 900
✳	21 600
○	24 600
●	27 800
Polymer flows	Entry in table 2, Virk (1971)
◪	9
▽	5
⊠	3
△	1

Patterson 1973). For clay minerals, however, the results were contradictory. Zandi (1967) claimed that drag reduction was observed with low concentrations of soft coal, fly ash, charcoal and clay, but the data in his paper were questioned by Radin *et al.* (1973). Kazanskij, Bruhl & Hinch (1974) measured pressure losses in pipe flow of a water/sand suspension when the clay mineral Bentonite was added. Bogue & Metzner (1963) did not find drag reduction in turbulent pipe flow of suspended Attapulgite. The author's mean flow measurements were performed with suspended clay minerals consisting of a mixture of Illite, Chlorite and Kaolinite (see § 2) and did demonstrate occurrence of drag reduction.

The experimental verification of drag reduction in a sea-water/clay-mineral suspension draws attention to the generating mechanism of this hydrodynamic phenomenon. According to recent investigations, viscoelastic solutions and

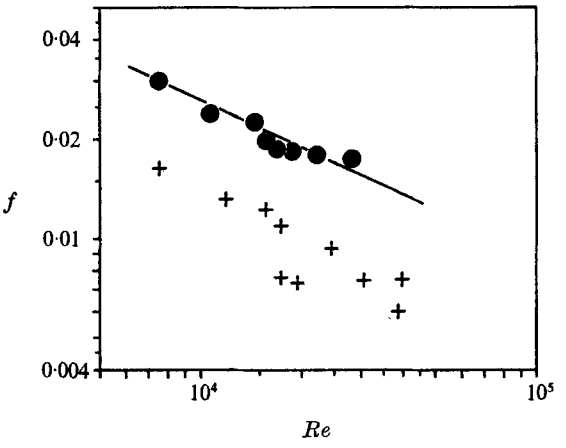

FIGURE 10. Coefficient of friction $f = 8(u_*/\bar{U})^2$ as function of equivalent pipe Reynolds number $Re = 4\bar{U}R/\nu$ (and suspension parameters) for experimental smooth open-channel flows. ●, pure water/sand bottom; ×, sea-water/clay suspension with mud bottom.

fibrous suspensions can exhibit drag reduction (see Radin *et al.* 1973). Furthermore, coarse dust particles in air, magnetic fields and flexible walls have been observed to cause turbulent-drag reduction (see references cited in Bark *et al.* 1975).

The way to model the mechanisms of drag reduction by various additives remains an open question (Oldroyd 1949; Lumley 1969; Virk 1971; Landahl 1973). Agglomeration of the clay particles is suggested as a possible cause of drag reduction occurring in clay suspension flow. Agglomeration of charged particles has already been considered as a mechanism giving rise to drag reduction (see Lumley 1969). It is proposed that not all types of aggregate cause drag reduction in view of the controversial results of clay suspension flow measurements cited in the literature. Depending on the crystal structure of the clay-mineral plates, various types of aggregate can be formed (see van Olphen 1963). The hypothesis is introduced that only those agglomerations which can change their shape under the influence of shear or vorticity in the turbulent flow cause drag reduction. Electrical processes other than agglomeration of charged suspended particles or charged particles and a charged bottom might well contribute to the mechanism causing drag reduction in a clay suspension. To consider such processes, more knowledge about the rheology of two-phase systems with suspended electrically charged particles is needed.

As a consequence of drag reduction in clay-mineral suspensions, results concerning the structure and dynamics of geophysical boundary layers have to be revised.

I should like to thank Dr Helmut Eckelmann and Dr Lorenz Magaard for many helpful discussions and Dr Gerold Siedler for his interest in my study. My thanks also go to the Forschungsanstalt für Wasserschall und Geophysik at Kiel for providing the sea-water resistant channel, constructed by Dipl.-Phys. I. Stender.

I am grateful to the Deutsche Forschungsgemeinschaft for financial support of this study. Frau Riese typed the manuscript, while Frau Mempel and Frau Schurbohm prepared the figures. This study was taken from my dissertation submitted to Kiel University in partial fulfilment of the requirements for my Ph.D. degree (1975).

REFERENCES

BAKEWELL, H. P. & LUMLEY, J. L. 1967 Viscous sublayer and adjacent wall region in turbulent pipe flow. *Phys. Fluids*, **10**, 1880.

BARK, F. H., HINCH, E. J. & LANDAHL, M. T. 1975 Drag reduction in turbulent flow due to additives: a report on Euromech 52. *J. Fluid Mech.* **68**, 129.

BOGUE, D. C. & METZNER, A. B. 1963 Velocity profiles in turbulent pipe flow. *Ind. & Engng Chem. Fund.* **2**, 143.

ECKELMANN, H. 1970 Experimentelle Untersuchungen in einer turbulenten Kanalströmung mit starken viskosen Wandschichten. *Mitt. Max-Planck-Inst. Strömungsforschung Aerodyn. Versuchsanstalt, Göttingen*, no. 48.

EINSTEIN, A. 1906 Neue Bestimmung der Moleküldimension. *Ann. Phys.* **19**, 289.

EINSTEIN, H. A. & KRONE, R. B. 1962 Experiments to determine modes of cohesive sediment transport in salt water. *J. Geophys. Res.* **67**, 1451.

FREY, H. R. & MCNALLY, G. J. 1973 Limitations of conical hot platinum film probes as oceanographic flow sensors. *J. Geophys. Res.* **78**, 1449.

FREYMUTH, P. 1967 Feedback control theory. *Rev. Sci. Instrum.* **38**, 677.

GUST, G. 1975 Untersuchungen zu sedimentologisch-hydrodynamischen Wechselwirkungen in einer turbulenten Tidenströmung mit suspendiertem Schlick (Meßprogramm 'Schliwe 1', Juli 1972). *Rep. Sonderforschungsbereich 95, Universität Kiel*, no. 11.

HINCH, E. J. & ZIABICKI, A. 1974 The mechanics of fluid suspensions and polymer solutions: a report on Euromech 49. *J. Fluid Mech.* **66**, 1.

HUNT, J. N. 1954 The turbulent transport of suspended sediment in open channels. *Proc. Roy. Soc.* A **224**, 322.

IPPEN, A. T. 1971 A. T. 1971 A new look at sedimentation in turbulent streams. *J. Boston Soc. Civ. Engrs*, **58**, 131.

JAYARAMAN, V. V. 1970 Resistance studies on smooth open channels. *Proc. A.S.C.E., J. Hydraul. Div.* **96**, 1129.

KAZANSKIJ, I., BRUHL, H. & HINCH, J. 1974 Influence of added fine particles on the flow structure and the pressure losses in sand–water-mixture. *Hydrotransport* **3**, *Golden, Colorado*, paper D2.

KEMP, P. H. & GRASS, A. J. 1967 The measurement of turbulent velocity fluctuations close to a boundary in open channel flow. *Proc. 12th Congress I.A.H.R.* **2**, 201.

KLATT, F. 1973 A study of systematic errors in measurements with the constant-temperature anemometer in high-turbulence flows with and without hot-wire signal linearization. *DISA Inf.* **14**, 25.

KRATKY, O., LEOPOLD, H. & STABINGER, H. 1969 Dichtemessung an Flüssigkeiten und Gasen auf 10^{-6} g/cm³ bei 0,6 cm³ Präparatvolumen. *Z. angew. Phys.* **27**, 273.

LANDAHL, M. T. 1973 Drag reduction by polymer addition. *Proc. 13th IUTAM Cong.* (ed. E. Becker & G. R. Mikhailov), p. 177. Springer.

LAUFER, J. 1954 The structure of turbulence in fully developed pipe flow. *N.A.C.A. Tech. Rep.* no. 1174.

LUMLEY, J. L. 1969 Drag reduction by additives. *Ann. Rev. Fluid Mech.* **1**, 367.

MCQUIVEY, R. S. & RICHARDSON, E. V. 1969 Some turbulence measurements in open-channel flow. *Proc. A.S.C.E., J. Hydraul. Div.* **95**, 209.

MIGNIOT, C. 1968 Etude des propriétés physiques de différents sédiments très fins et leur comportements sous des actions hydrodynamiques. *Houille Blanche*, **23**, 591.

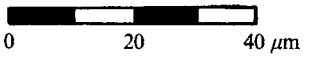

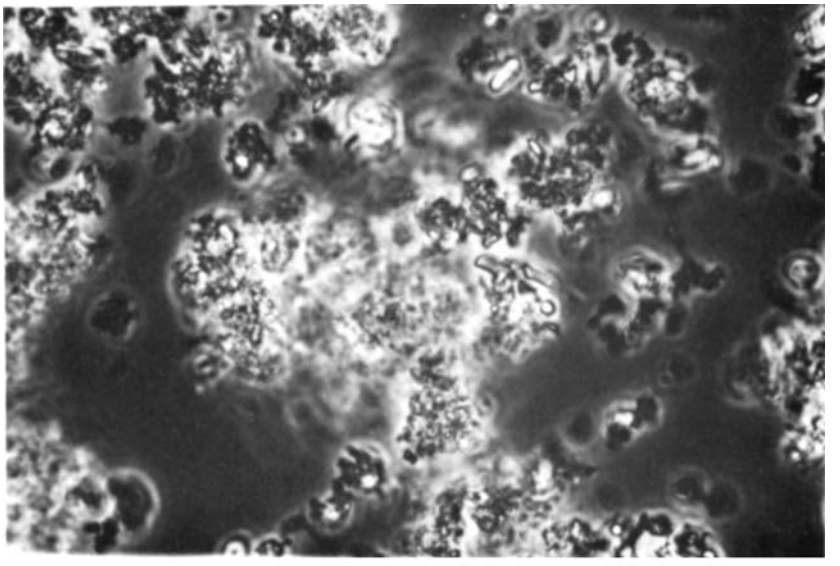

(*a*)

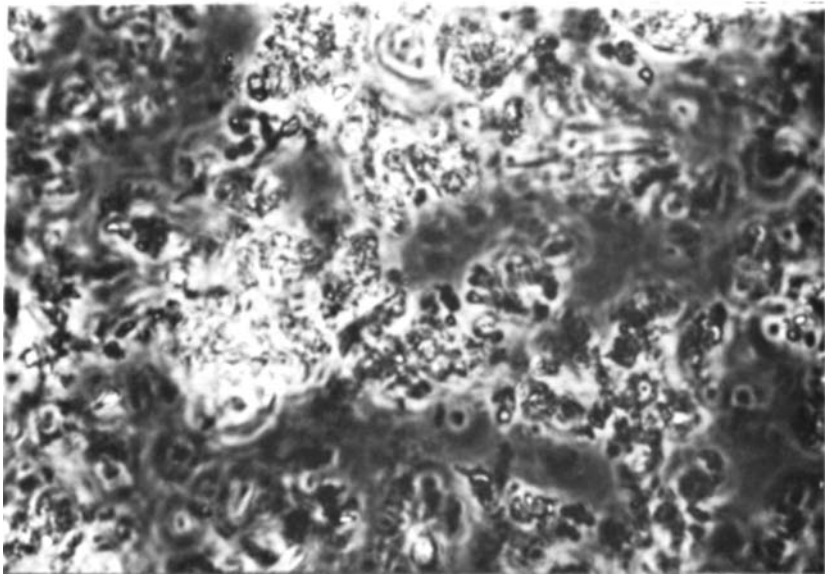

(*b*)

FIGURES 5(*a*, *b*). For legend see plate 2.

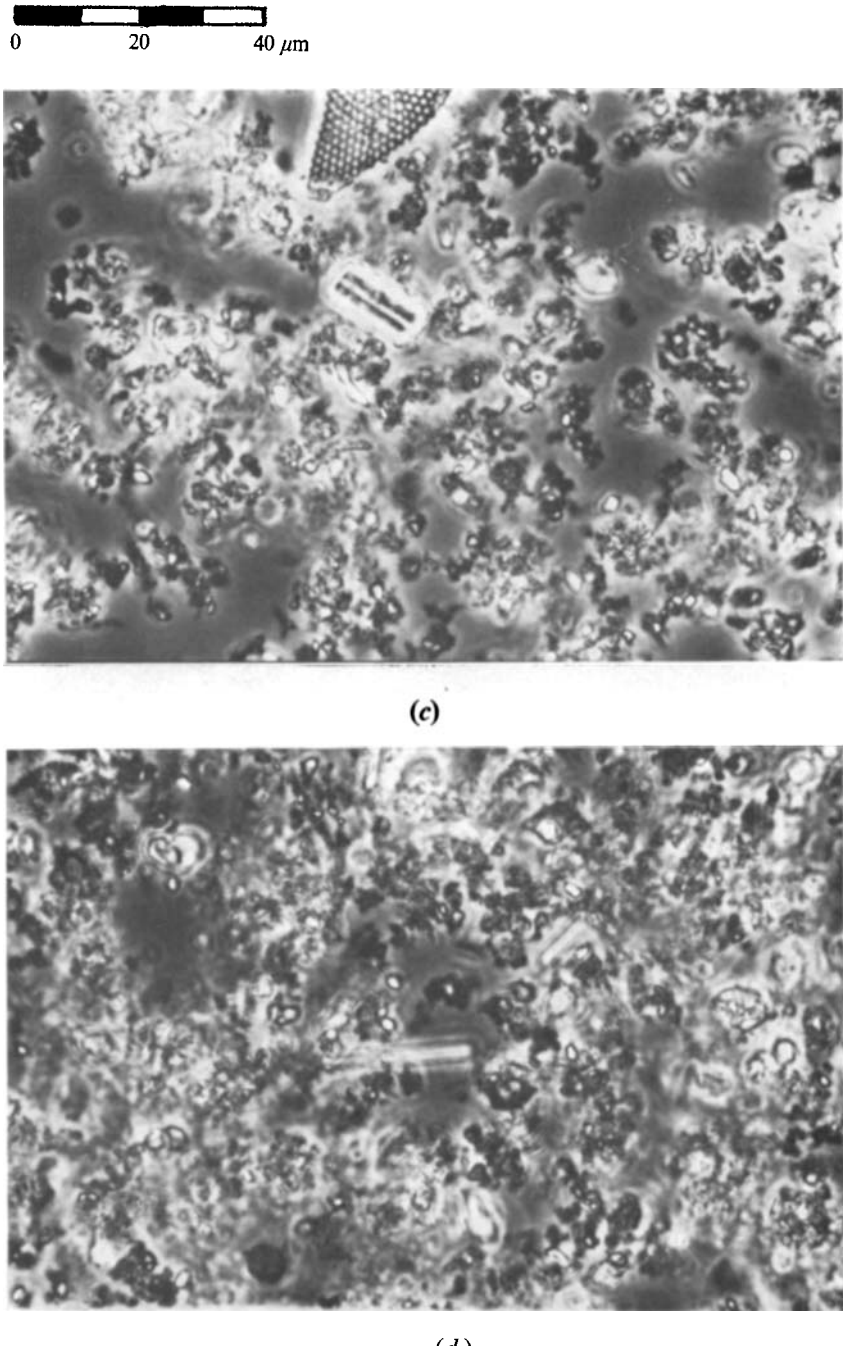

FIGURE 5. Microphotos from the phase contrast microscope.

	Reynolds number Re_U	Height of sample above bottom (cm)
(*a*)	13 100	1
(*b*)	13 100	2
(*c*)	8 500	3
(*d*)	21 600	3